

Review

Stability of Halloysite, Imogolite, and Boron Nitride Nanotubes in Solvent Media

Lorenzo Lisuzzo ¹ , Giuseppe Cavallaro ¹, Giuseppe Lazzara ^{1,*} , Stefana Milioto ¹,
Filippo Parisi ¹  and Yuriy Stetsyshyn ² 

¹ Dipartimento di Fisica e Chimica, Università degli Studi di Palermo, 90128 Palermo, Italy; lorenzo.lisuzzo@unipa.it (L.L.); giuseppe.cavallaro@unipa.it (G.C); stefana.milioto@unipa.it (S.M.); filippo.parisi@unipa.it (F.P.)

² Department of Organic Chemistry, Lviv Polytechnic National University, 79013 Lviv, Ukraine; yrstecushun@ukr.net

* Correspondence: giuseppe.lazzara@unipa.it; Tel.: +39 09123897962

Received: 28 May 2018; Accepted: 27 June 2018; Published: 30 June 2018



Featured Application: The review is focused on the stabilization of nanotubular materials in solvent media. This aspect is a key starting point for any application of nanotube-based formulations for pharmaceutical and industrial applications.

Abstract: Inorganic nanotubes are attracting the interest of many scientists and researchers, due to their excellent application potential in different fields. Among them, halloysite and imogolite, two naturally-occurring aluminosilicate mineral clays, as well as boron nitride nanotubes have gained attention for their proper shapes and features. Above all, it is important to reach highly stable dispersion in water or organic media, in order to exploit the features of this kind of nanoparticles and to expand their applications. This review is focused on the structural and morphological features, performances, and ratios of inorganic nanotubes, considering the main strategies to prepare homogeneous colloidal suspensions in various solvent media as special focus and crucial point for their uses as nanomaterials.

Keywords: colloidal stability; nanoparticle dispersion; halloysite; imogolite; boron nitrides; nanotubes

1. Introduction

Since carbon nanotubes were discovered in 1991 [1], the nanotube structure has garnered interest and has been widely researched in other types of particles, like metal nanotubes [2,3], oxide nanotubes [4,5], boron nitride nanotubes [6,7] and nanotubular clays, to study the characteristics of tunable chemistry, surface area, and porosity.

The need to reach homogeneous particles dispersion in different solvent media represents one of the main conditions for the use and applicability of those systems [8]. With this aim, this review will be focused on the colloidal stability of inorganic nanotubes, as well as on the most used strategies to prepare well-dispersed suspensions. In particular, these aspects will be investigated for halloysite nanotubes (HNTs) [8], imogolite nanotubes (INTs) [9], and boron nitride nanotubes (BNNTs) [10].

Halloysite nanotubes are composed of a silicon oxygen tetrahedron and alumina oxygen octahedrons forming a kaolinite-like sheet that rolls up, giving the clay its own hollow tubular structure (Figure 1a) [11,12]. Since the lumen and the external surface are chemically different, they are positive and negative in water, respectively, in the 2–8 pH range [13]. HNT size varies with respect to the natural origin, ranging from 0.5 to 1.5 μm in length, within 50–70 nm for the outer nanotube diameter

and 10–20 nm for the internal diameter [14]. Moreover, they have biocompatibility [15] and show no toxicity *in vivo* [16] and *in vitro* [17]. These characteristics make HNTs excellent smart materials for the most diverse applications—for example: food packaging [18–20], drug delivery [21–26], environment remediation and wastewater treatment [27], cultural heritage [28–32], and additives for enhancing the performances of polymers [14,33].

Imogolite, firstly observed in volcanic soils, is another natural aluminosilicate whose shape is nanotubular, with an external diameter of about 2 nm; its length can be expressed in micrometers [34]. INTs are always arranged into bundles, so it is not possible to observe a single nanotube, but rather a network of bundles (Figure 1b) [35]. Their structure, proposed by Cradwick in 1972, is very similar to halloysite, namely a layer of orthosilicate tetrahedra overlapping a layer with an aluminum in a dioctahedral configuration [36]. INTs are considered the clay counterpart of carbon nanotubes, and they are very similar if dimensions, aspect ratios, and rigidity are considered [9]. Moreover, imogolite nanotubes are easily synthesized using hydrothermal techniques, without purification steps to do post-synthesis, and they form stable colloidal suspensions in aqueous solvents [34,37].

The good monodispersity of INTs has motivated researchers to investigate their formation process. Preparation routes for imogolite were developed very quickly. For instance, the possibility of controlling their structure and chemical nature makes them very interesting nano-platforms for various applications [37].

BNNTs were predicted in 1994 [38], and first prepared by Chopra et al. [39] in 1995 as carbon nanotube inorganic analogs, by alternating boron and nitrogen instead of carbon, almost without changing the atomic spacing of the graphite-like sheet [10,38]. The key parameters that influence both the length and size of BNNTs are temperature, catalyst, and boron precursor, as well as duration of the heating process [10]. The external diameter varies from 4 to 300 nm, usually reaching 30–100 nm, and the tubes' lengths are in the range of 500 nm to 1 mm, usually 5–10 μm [10]. Moreover, by changing the condition of synthesis, a single-walled BNNT, a double-walled BNNT, or a multi-walled BNNT can be prepared [40]. Although they are very similar to CNTs, BNNTs show greater mechanical (Young's modulus of 1.2 TPa) [41], and excellent chemical [42] and electrical properties [43]. One of the critical points for the applications of BNNTs, as well for CNTs, is their very poor dispersibility in water and apolar media. Being hydrophobic, BNNTs tend to aggregate and precipitate in about 1 h in aqueous media [44]. Therefore, they can be exploited in the biological field after an appropriate noncovalent [45,46] or covalent [47] modification, which can increase their dispersibility in water. BNNTs were used as smart materials [7], drug [47] and gene delivery systems [48], biomaterials [49], sensory systems [50], as well as hydrogen storage [51].

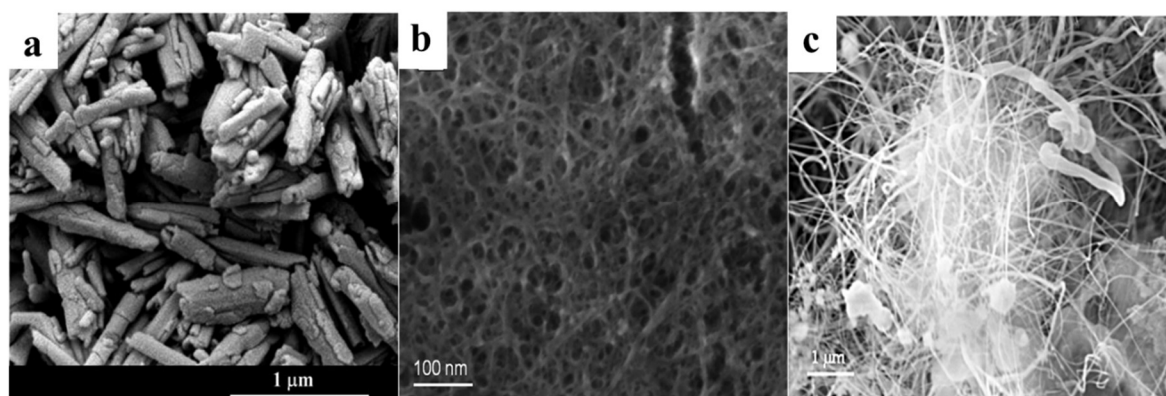


Figure 1. SEM images of (a) halloysite, (b) imogolite and (c) boron nitride nanotubes. Adapted from References [7,35,52].

2. Halloysite Nanotubes

2.1. Colloidal Stability in Water

The colloidal stability of HNTs is a crucial aspect that has been investigated with the aim of improving nanoparticle use and range through several possible applications [8]. HNTs' aqueous dispersions can form liquid crystalline phases when high concentrations are approached [53]. Moreover, the transition can be controlled by pH, providing an interesting system for obtaining birifrangent materials under controlled chemical stimuli [53]. In light of that, different strategies for the manipulation of chemico-physical properties into aqueous media are pursued by the most appropriate functionalization of halloysite internal or external surfaces by electrostatic interactions with differently charged surfactants or polyelectrolytes.

Bertolino et al. [54] reported studies on the adsorption of three biopolymers that possess a different charge—namely positive chitosan, neutral hydroxypropyl cellulose (HPC), and negative pectin—onto halloysite nanotube surfaces in an aqueous environment. It was found that the dispersion stability depends on the charge of particles and their dimensions, as well on the viscosity and inter-particle interactions. For instance, the ζ -potential values are not deeply modified by adding the nonionic HPC; meanwhile they are shifted toward more positive or more negative values by the addition of charged biopolymers, namely chitosan and pectin, respectively [54]. Generally, ζ -potential experiments are conducted to evaluate the surface properties and stability of functionalized nanoparticles, in order to understand if the charge density of both HNTs and polymers can influence the precipitation process. It was observed that HPC strongly delays sedimentation; meanwhile, chitosan and pectin stabilize nanotube dispersion at acidic and basic conditions, respectively. Pectin interacts with the HNTs' positive lumen and it decreases the HNTs' negative net charge. Chitosan, however, interacts on the outer surface. The HPC mechanism is completely different, because it is adsorbed and it creates a steric barrier that avoids agglomeration and settling [54].

Lee et al. [55] reported the preparation of HNT-based supramolecular complexes by the wrapping of DNA onto halloysite. It was observed that HNTs become highly dispersible in water after their interaction with DNA, because the phosphate groups of DNA are re-orientated and can interact with the silica groups on the external surface of HNTs. Most likely, the enhanced colloidal stability is due to the neutralization of the inner positive charge, leading to an increase of the net negative ζ -potential and particle–particle repulsions. These findings are confirmed by more recent studies on anionic surfactants and bio-polyanions (pectins) [54,56].

The effect on the colloidal stability of halloysite nanotubes has been also studied, considering the functionalization with thermosensitive polymers, namely poly(*N*-isopropylacrylamide) (PNIPAM) [57,58]. It was observed that PNIPAM interacted with the external surface of HNT and PNIPAM–NH₂ (amine terminated poly(*N*-isopropylacrylamide)) was adsorbed onto the external surface. Moreover, halloysite nanotubes changed their properties within the polymer/HNTs in comparison with the neat clay, thus indicating a transferring of the thermos-responsiveness from polymers to halloysite in the hybrid system [57]. Furthermore, since the dispersions were stable only under the “critical temperature”, this allowed for preparing systems where the temperature can be tuned in order to have external stimuli-responsive solubilization and delivery, providing a biocompatible and thermosensitive material for the targeted release of active species [58].

Amphiphilic molecules are often used to stabilize nanoparticle dispersions, exploiting their functional groups. The choice of the surfactant in terms of the headgroup charge is a key factor, and it has an important effect on the colloidal stability of halloysite because of its differently charged surfaces.

For instance, it has been demonstrated that the adsorption of surfactants that are negatively charged (e.g., sodium alkanoates) onto the internal surface of the nanotubes increases their overall negative charge, and thus enhances both electrostatic repulsions and colloidal stability (Figure 2) [56,59].

The change of the ζ potential, which becomes more negative, predicts a better dispersibility of the hybrid materials in comparison with the neat clay. The sedimentation process is strongly slowed down by the surfactants [59].

According to the DLVO (Derjaguin-Landau-Verwey-Overbeek) theory, colloidal stability is influenced by the balance between attractive and repulsive van der Waals forces coming from the double layer that surrounds each particle [60], meaning that experimental results are consistent with the theory.

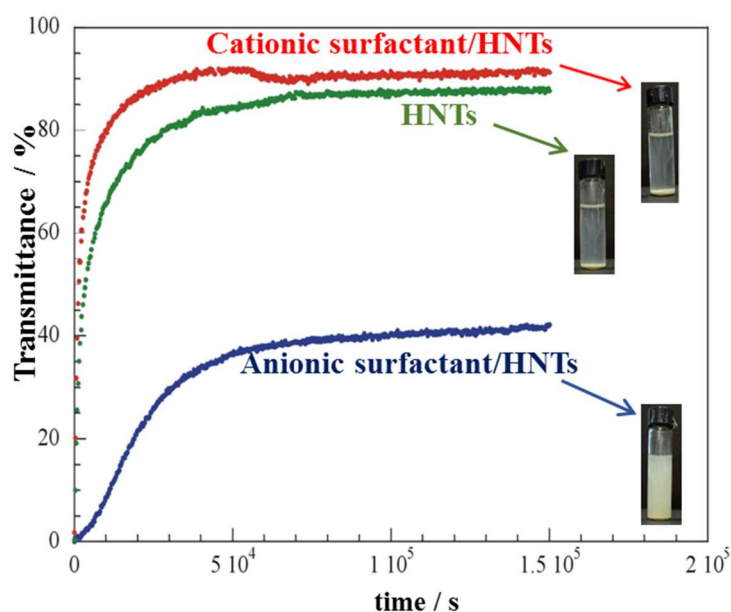


Figure 2. Halloysite nanotubes (HNTs) and surfactant-functionalized HNT dispersions (1 wt %) in water: photographs and transmittance as a function of time. Adapted from [56].

Moreover, the structure of neat HNTs and negatively charged surfactant-functionalized nanotubes were studied by small angle neutron scattering [52]. The importance of both the structural organization of the surfactants and their headgroup was shown. In particular, it was noted that sodium dodecanoate is organized in a densely packed, multilayer structure within the halloysite cavity, and is promoted by the carboxylate groups, as seen from a correlation peak in SANS (Small Angle Neutron Scattering) [52].

Finally, these inorganic, micelles-like hybrid materials can be used to solubilize and deliver species of a different nature in water, thus exploiting their sustainable and biocompatible properties [52,56,59].

It was also found that perfluoroalkylated surfactants, when adsorbed at the internal surface, created stable suspensions, and these systems can be exploited as nanocontainers of non-foaming oxygen in aqueous media for gas delivery by external stimuli [61].

More interestingly, it was shown that the concentration effect was negligible and that the hybrid materials did not associate; however, nanotubes diffuse as single particles [61].

Lun et al. [62] reported a method where sodium dodecyl sulfate (SDS) was used to prepare uniform and stable halloysite nanotubes dispersions. The ζ -potential values of an HNTs/SDS system became more negative than those of the neat clay, indicating that SDS is adsorbed on the inner surface, enhancing the dispersibility by electrostatic effect. It was observed that the dispersibility is not effected by the content of the dispersant, thus confirming the saturation effect.

2.2. Colloidal Stability in Organic Media

Another crucial aspect is the preparation of stable colloidal dispersions of halloysite nanotubes in organic media. Chang et al. [63] prepared a complex of amylose and HNT by co-assembly in a

solid state. In particular, it was found that the amylose interacts with the outer surface of HNTs, wrapping them. The stability of pristine nanotubes and amylose-HNT dispersions in DMSO/H₂O were observed for 24 h, and the precipitation of HNT occurred at 0 h [63]; whereas, since the solution of DMSO/H₂O is a good dispersant for the organic moiety, the amylose-HNT was well dispersed in the solution, and no precipitation was found for 24 h [64]. This was most likely due to the interactions between amylose and the external surface of HNTs [63]. Literature also reports another strategy to obtain stable colloidal suspensions, which is the preparation of inorganic reverse micelles in non-aqueous media based on halloysite nanotubes and cationic surfactants [65]. It is known that a reverse micelle is constituted by a hydrophobic shell and a hydrophilic cavity, which create an aqueous nano-droplet in a nonpolar medium. Cationic surfactants interact with the negative outer surface of HNTs, thus creating nanoparticles with a hydrophobic jacket and a hydrophilic cavity. The action of the colloidal stability of the obtained hybrid materials was investigated in solvents with different polarity [65]. Firstly, it was observed that the length chain of the surfactant strongly influences the charge of modified HNTs. For instance, when the tail length increases, the same happens to the ζ potential of the hybrid materials, due to the strong hydrophobic interaction between tails, as evidenced by FTIR [56]. Moreover, the hybrids present faster dynamics compared to the neat nanotubes, as evidenced by DLS (Dynamic Light Scattering) measurements in chloroform, thus reflecting the enhancement of electrostatic repulsions. The external surface of nanotubes is more hydrophobic, due to the presence of the surfactant, resulting in an increase of the colloidal stability of the nanotubes in nonpolar solvents [65]. In a few words, this procedure allows the fabricating of eco-compatible reverse micelles with different dispersibility in organic media and tunable hydrophobic/hydrophilic interfaces, thus available for industrial or biological applications.

3. Imogolite

Concerning imogolite nanotubes, although their formation mechanism has been extensively investigated and described in recent literature [66], their stability in aqueous suspension was not deeply investigated. On the other hand, Paineau et al. [9] firstly observed that INTs show a liquid-crystal phase, columnar in particular, at low concentrations ($\approx 0.3\%$) with low visco-elasticity and that is aligned under an electric field.

As expected, INT suspensions form a nematic phase at lower concentrations [67]. Contrarily, the columnar phase, which can be seen in suspensions of other rod-like particles, was only observed at large volume fractions (10–70%) [68–70]. Meanwhile the columnar phase of INTs is presented at concentrations that are two orders of magnitude lower (Figure 3) [9].

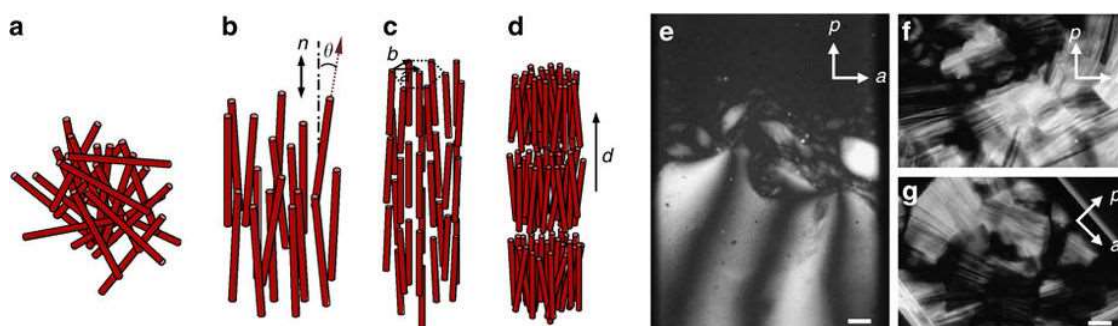


Figure 3. Schemes of (a) isotropic, (b) nematic, (c) columnar, and (d) smectic phases in imogolite suspensions. Photographs of (e) both isotropic and nematic phases in sedimented spindle-shaped nematic droplets; and (f, g) the columnar phase, obtained with single-walled Si-imogolite nanotube (INT) suspensions. Scale bar, 200 nm. Adapted from [9].

Such a difference is most likely due to the high aspect ratio of imogolite, which favors the nematic phase [67]. The large intensity of the electrostatic repulsions between charged linear objects is strongly evidenced by the ordered positions of the charged INT, which stabilizes the columnar phase at very low concentrations [9].

These results could present important implications for the physics of suspensions of charged rod-shaped nanoparticles, and could be used for the preparation of ordered nanocomposites, as well for biophysics, in order to understand the behavior of rod-like biopolymers suspensions.

Moreover, it was observed that imogolite forms sediments at an alkaline pH, even if the net charge is highly negative, and this leads to fibrous particle aggregation to form thick bundles [71]. To clarify this aspect, Ma and Karube [72] measured the charge features of INT by calculating the intensity of the electric field at the external surface, considering the model of imogolite structure and the Gauss' law.

It was calculated that the field intensity, due to the charge at the external surface of INTs, is half that at the internal surface. It was impossible to explain the flocculation, because the cation exchange capability (CEC) of imogolite was high under alkaline conditions. For instance, assuming cation distribution inside the tube, or inner cation exchange, the measured CEC would correspond to the negative charge at the inner surface, and the electric field intensity at the external surface would become half that at the internal surface [72]. This means that the electric field, due to the negative charges, would be balanced by the counter-ions that entered the tube, and the external surface would be neutral, thus explaining that imogolite flocculates at alkaline pH and its dispersed at the point of zero net charge, or at pH = 6.0 [72].

4. Boron Nitride Nanotubes

To improve dispersion stability, numerous methods to functionalize BNNTs were used [10,45,73]. These methods can be organized into three groups: (1) noncovalent, (2) covalent modifications, and (3) alternation in BNNTs (fabrication of defect sites, insertion of the amino groups, and transformation of the amino groups) (Figure 4).

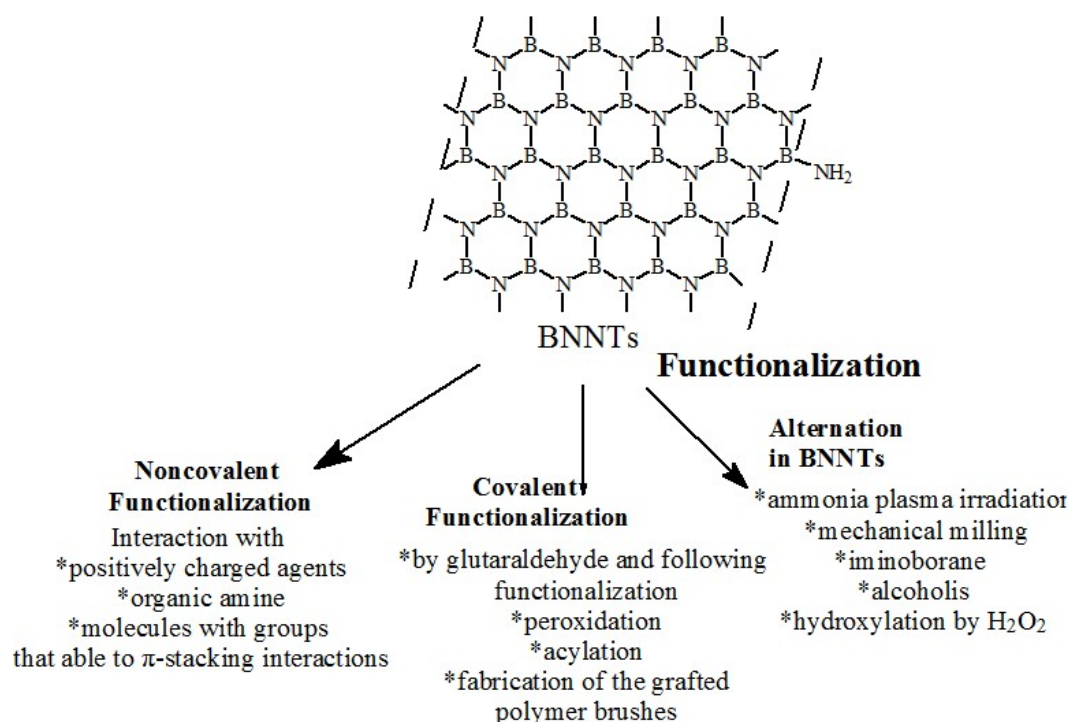


Figure 4. Different approaches for functionalization of the boron nitride nanotubes (BNNTs).

Noncovalent reactions are the most frequently used approach for the surface functionalization of BNNTs [73]. However, only positively charged agents (e.g., poly-L-lysine and poly-ethyleneimine), organic amines, or chemical species able to make π -stacking and hydrophobic interactions showed good results [73]. Synthetic structures with aromatic rings (2-naphthalenecarboxylic acid, 9-anthracenecarboxylic acid, 1-pyrenecarboxylic acid, 1-aminopyrene, and 1-hydroxypyrene) [74] and polymers containing aromatic subunits, polyaniline, poly(p-phenyleneethynylene), polythiophene, poly(xylydienetetrahydrothiophene) and poly(sodium styrene sulfonate) [73,75] interacted with the sidewall of BNNTs via π - π stacking and created stable dispersions. It was shown that poly(p-phenylene) derivatives have the most interesting potential to disperse BNNTs among studied polymers [75].

Another simple way to prepare stable colloidal dispersions of BNNTs in organic solution or aqueous media is to obtain boron nitride nanotubes with NH_3 or organic amines [76] or amino acids (glycine), and coat them subsequently with biopolymers [77]. The glycine has two roles: its amine group interacts with the B-sites of nanotubes, binding with them; meanwhile, its carboxylic acid group is an ionic site for anchoring polyelectrolytes. Unexpectedly, BNNTs were effectively dispersed in water using arabic gum (hydrophilic polymer), where the hydrophobic part of the polymers had strong hydrophobic interactions with BNNTs and the hydrophilic part was exposed to interactions with water molecules [78]. Other examples of the fabrication of the stable BNNT dispersions are modification of the BNNTs, using peptides [79], nucleotide [80], DNA [81], doxorubicin and folate [82], and lipids [83]. The most stable dispersions in water were obtained for the flavin mononucleotide, a derivative of vitamin B₂ containing an aromatic structure interacting with BNNT via π - π stacking [80]. In addition, flavin mononucleotide-functionalized BNNTs showed high visible light emission, and were stable for different pH and temperature values. A new approach to disperse the BNNTs was recently demonstrated [6], in this case via a layer-by-layer deposition of hydroxylated BNNTs with polyelectrolytes onto *Saccharomyces cerevisiae* cells.

Different methods of covalent modification of BNNTs have been developed to create colloidal dispersions in both aqueous media and organic solvents. This functionalization can be done by exploiting the $-\text{NH}_2$ and $-\text{OH}$ groups of boron atoms [46,84–86]. Covalent modification of the hydroxylated BNNTs with glutaraldehyde, followed by functionalization with oligonucleotides [87] and carbohydrates [88] are described. Zettl developed a new functionalization route by linking stearoyl chloride with amino groups onto BNNTs [84]. A similar approach was realized with hydroxylated BNNTs esterified by perfluorobutyric acid or a thioglycolic acid [88]. Another easy approach for covalent derivatization of nanotubes with organic peroxides was proposed [89], and the functionalized BNNTs were able to form the stable dispersion in chloroform.

Nowadays, one of the most interesting procedures for nanomaterial functionalization is to prepare grafted polymer brushes [7,90] (Figure 5a). In this route, the nanotubes are covalently functionalized with polymer brushes through surface polymerization. In particular, BNNTs were covalently modified with hydrophobic polystyrene or polyglycidyl methacrylate polymer brushes [90]. The modified nanotubes displayed high dispersibility in a large number of organic media. In the work of Kalay et al. [7], BNNTs functionalized with the thermo-responsive poly(*N*-isopropylacrylamide) (PNIPAM) were fabricated, and were dispersible in water (Figure 5b). It was also shown that the hydrodynamic radius of these systems decreased two-fold at around 32 °C (Figure 5c). In addition, BNNTs were functionalized by other grafted polymer brushes, similar to other works [91,92].

The modification of nanotubes on their amine groups is widely used, because the amine groups exist at the ends and as defects of BNNTs. Moreover, other $-\text{NH}_2$ groups were also created on the nanotube surfaces with ammonia plasma irradiation [84]. Amine-functionalized BNNTs after sonication in chloroform exhibit significantly better dispersibility than pristine BNNTs. Other mechanisms of functionalization by amine groups use mechanical milling of the boron nitride nanosheets [93] or iminoborane, which increases the defects density due to cleavage of B–N bonds and

to the expansion of BN rings [94]. In addition, a prospective method to create stable dispersion in water is the hydroxylation of BNNTs in H_2O_2 solution for 48 h at 110 °C [86,87].

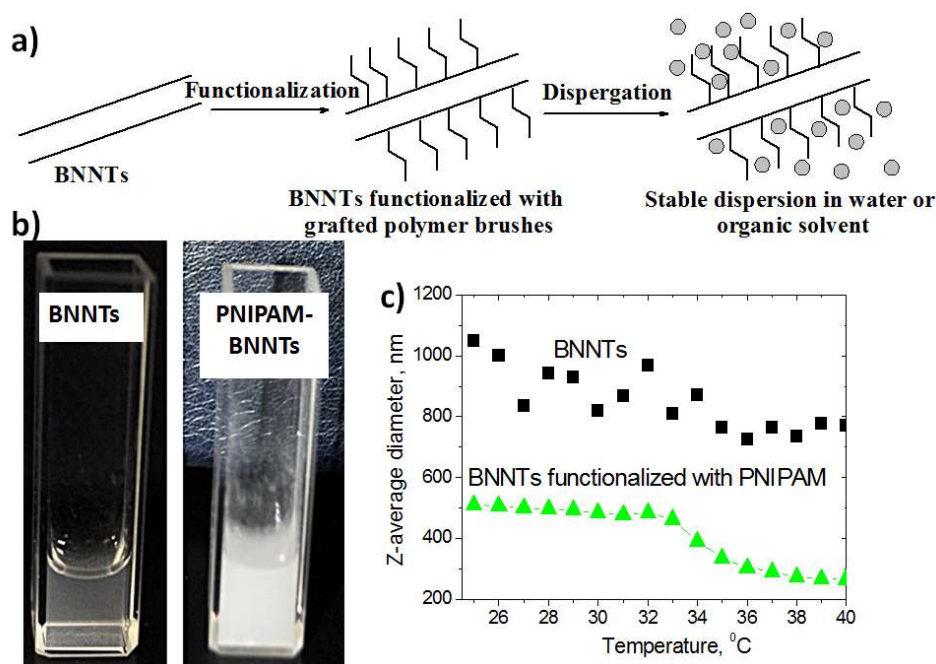


Figure 5. Fabrication of stable dispersion of the functionalized BNNTs (a), supernatants obtained after the water suspensions of native and PNIPAM-functionalized BNNT centrifugation (b), and Z-average diameters of the neat and PNIPAM-functionalized BNNTs at different temperatures (c). Adapted from [7].

5. Conclusions and Perspectives

It is clear the importance of nanotubular inorganic structures for their characteristics of high surface ratios, porosity, and tunable chemistry. Halloysite, imogolite, and boron nitride nanotubes are among the prospective tubular materials for industrial applications. In particular, they are considered safe materials for living organisms. Although they present a similar morphology, their chemical structure and properties are different. Chemical composition of HNTs and INTs are very similar; the surface chemistry is dominated by hydroxyl groups that make them hydrophilic. In the contrast, native BNNTs are superhydrophobic, and cannot be dispersed in most organic solvents or in aqueous media. BNNTs show greater mechanical properties (Young's modulus of 1.22 TPa) than HNTs and INTs (Young's modulus of 140–390 GPa). Another interesting aspect is the pH effect on surface charge. The dielectric properties of aluminum and silicon oxides in HNTs and INTs are different. Because these nanotubes undergo ionization in aqueous media in an opposite way, they generate tubes with oppositely charged inner and outer surfaces. Information on BNNT ionization is limited; in relation to chemical structure, we can assume that BNNTs can be ionized at a low pH, but this aspect should be investigated in detail. In addition, HNTs and INTs can be easily modified using hydroxyl groups on the outer surface, while BNNTs are chemically inert enough.

In this review, we report the main aspects of the colloidal stability of hollow-shaped nanoparticles in both aqueous and organic media, as well as the main strategies to prepare homogeneous and stable suspensions ranging from selective functionalization with charged molecules like polymers, biopolymers, and surfactants to pH dependence in water. These are crucial points for the preparation of a new class of smart hybrid nanomaterials with a wide class of applications, like drug delivery, catalysis, food packaging, environmental treatment, and cultural heritage.

Author Contributions: Writing-Original Draft Preparation, L.L., G.C., F.P., Y.S.; Writing-Review & Editing, G.L.; Supervision, S.M.

Funding: The work was financially supported by the University of Palermo.

Conflicts of Interest: The authors declare that they have no conflicts of interest with this work.

References

1. Iijima, S. Helical microtubules of graphitic carbon. *Nature* **1991**, *354*, 56–58. [[CrossRef](#)]
2. Sun, J.; Wang, J.; Li, Z.; Yang, Z.; Yang, S. Controllable synthesis of 3D hierarchical bismuth compounds with good electrochemical performance for advanced energy storage devices. *RSC Adv.* **2015**, *5*, 51773–51778. [[CrossRef](#)]
3. Yang, G.; Yang, X.; Yang, C.; Yang, Y. A reagentless amperometric immunosensor for human chorionic gonadotrophin based on a gold nanotube arrays electrode. *Colloids Surf. Physicochem. Eng. Asp.* **2011**, *389*, 195–200. [[CrossRef](#)]
4. Lai, Y.; Huang, Y.; Wang, H.; Huang, J.; Chen, Z.; Lin, C. Selective formation of ordered arrays of octacalcium phosphate ribbons on TiO₂ nanotube surface by template-assisted electrodeposition. *Colloids Surf. B Biointerfaces* **2010**, *76*, 117–122. [[CrossRef](#)] [[PubMed](#)]
5. Xu, S.; Ng, J.; Zhang, X.; Bai, H.; Sun, D.D. Adsorption and photocatalytic degradation of Acid Orange 7 over hydrothermally synthesized mesoporous TiO₂ nanotube. *Colloids Surf. Physicochem. Eng. Asp.* **2011**, *379*, 169–175. [[CrossRef](#)]
6. Emanet, M.; Fakhrullin, R.; Çulha, M. Boron Nitride Nanotubes and Layer-By-Layer Polyelectrolyte Coating for Yeast Cell Surface Engineering. *Chem. Nano. Mat.* **2016**, *2*, 426–429. [[CrossRef](#)]
7. Kalay, S.; Stetsyshyn, Y.; Lobaz, V.; Harhay, K.; Ohar, H.; Çulha, M. Water-dispersed thermo-responsive boron nitride nanotubes: Synthesis and properties. *Nanotechnology* **2016**, *27*, 035703. [[CrossRef](#)] [[PubMed](#)]
8. Lazzara, G.; Cavallaro, G.; Panchal, A.; Fakhrullin, R.; Stavitskaya, A.; Vinokurov, V.; Lvov, Y. An assembly of organic-inorganic composites using halloysite clay nanotubes. *Curr. Opin. Colloid Interface Sci.* **2018**, *35*, 42–50. [[CrossRef](#)]
9. Paineau, E.; Krapf, M.-E.M.; Amara, M.-S.; Matskova, N.V.; Dozov, I.; Rouzière, S.; Thill, A.; Launois, P.; Davidson, P. A liquid-crystalline hexagonal columnar phase in highly-dilute suspensions of imogolite nanotubes. *Nat. Commun.* **2016**, *7*, 10271. [[CrossRef](#)] [[PubMed](#)]
10. Kalay, S.; Yilmaz, Z.; Sen, O.; Emanet, M.; Kazanc, E.; Çulha, M. Synthesis of boron nitride nanotubes and their applications. *Beilstein J. Nanotechnol.* **2015**, *6*, 84–102. [[CrossRef](#)] [[PubMed](#)]
11. Massaro, M.; Amorati, R.; Cavallaro, G.; Guernelli, S.; Lazzara, G.; Milioto, S.; Noto, R.; Poma, P.; Riela, S. Direct chemical grafted curcumin on halloysite nanotubes as dual-responsive prodrug for pharmacological applications. *Colloids Surf. B Biointerfaces* **2016**, *140*, 505–513. [[CrossRef](#)] [[PubMed](#)]
12. Ferrante, F.; Armata, N.; Lazzara, G. Modeling of the Halloysite Spiral Nanotube. *J. Phys. Chem. C* **2015**, *119*, 16700–16707. [[CrossRef](#)]
13. Yang, Y.; Chen, Y.; Leng, F.; Huang, L.; Wang, Z.; Tian, W. Recent Advances on Surface Modification of Halloysite Nanotubes for Multifunctional Applications. *Appl. Sci.* **2017**, *7*, 1215. [[CrossRef](#)]
14. Makaremi, M.; Pasbakhsh, P.; Cavallaro, G.; Lazzara, G.; Aw, Y.K.; Lee, S.M.; Milioto, S. Effect of Morphology and Size of Halloysite Nanotubes on Functional Pectin Bionanocomposites for Food Packaging Applications. *ACS Appl. Mater. Interfaces* **2017**, *9*, 17476–17488. [[CrossRef](#)] [[PubMed](#)]
15. Kryuchkova, M.; Danilushkina, A.; Lvov, Y.; Fakhrullin, R. Evaluation of toxicity of nanoclays and graphene oxide in vivo: A Paramecium caudatum study. *Environ. Sci. Nano* **2016**, *3*, 442–452. [[CrossRef](#)]
16. Fakhrullina, G.I.; Akhatova, F.S.; Lvov, Y.M.; Fakhrullin, R.F. Toxicity of halloysite clay nanotubes in vivo: A Caenorhabditis elegans study. *Environ. Sci. Nano* **2015**, *2*, 54–59. [[CrossRef](#)]
17. Lvov, Y.; Abdullayev, E. Functional polymer–clay nanotube composites with sustained release of chemical agents. *Prog. Polym. Sci.* **2013**, *38*, 1690–1719. [[CrossRef](#)]
18. Biddeci, G.; Cavallaro, G.; Di Blasi, F.; Lazzara, G.; Massaro, M.; Milioto, S.; Parisi, F.; Riela, S.; Spinelli, G. Halloysite nanotubes loaded with peppermint essential oil as filler for functional biopolymer film. *Carbohydr. Polym.* **2016**, *152*, 548–557. [[CrossRef](#)] [[PubMed](#)]

19. Bertolino, V.; Cavallaro, G.; Lazzara, G.; Merli, M.; Milioto, S.; Parisi, F.; Sciascia, L. Effect of the Biopolymer Charge and the Nanoclay Morphology on Nanocomposite Materials. *Ind. Eng. Chem. Res.* **2016**, *55*, 7373–7380. [[CrossRef](#)]
20. Gorrasi, G.; Pantani, R.; Murariu, M.; Dubois, P. PLA/Halloysite Nanocomposite Films: Water Vapor Barrier Properties and Specific Key Characteristics. *Macromol. Mater. Eng.* **2014**, *299*, 104–115. [[CrossRef](#)]
21. Massaro, M.; Lazzara, G.; Milioto, S.; Noto, R.; Riela, S. Covalently modified halloysite clay nanotubes: Synthesis, properties, biological and medical applications. *J. Mater. Chem. B* **2017**, *5*, 2867–2882. [[CrossRef](#)]
22. Lvov, Y.M.; DeVilliers, M.M.; Fakhrullin, R.F. The application of halloysite tubule nanoclay in drug delivery. *Expert Opin. Drug Deliv.* **2016**, *13*, 977–986. [[CrossRef](#)] [[PubMed](#)]
23. Fakhrullin, R.F.; Lvov, Y.M. Halloysite clay nanotubes for tissue engineering. *Nanomedicine* **2016**, *11*, 2243–2246. [[CrossRef](#)] [[PubMed](#)]
24. Liu, M.; Zhang, Y.; Wu, C.; Xiong, S.; Zhou, C. Chitosan/halloysite nanotubes bionanocomposites: Structure, mechanical properties and biocompatibility. *Int. J. Biol. Macromol.* **2012**, *51*, 566–575. [[CrossRef](#)] [[PubMed](#)]
25. Liu, M.; Wu, C.; Jiao, Y.; Xiong, S.; Zhou, C. Chitosan-halloysite nanotubes nanocomposite scaffolds for tissue engineering. *J. Mater. Chem. B* **2013**, *1*, 2078–2089. [[CrossRef](#)]
26. Cavallaro, G.; Lazzara, G.; Milioto, S.; Parisi, F.; Evtugyn, V.; Rozhina, E.; Fakhrullin, R. Nanohydrogel Formation within the Halloysite Lumen for Triggered and Sustained Release. *ACS Appl. Mater. Interfaces* **2018**, *10*, 8265–8273. [[CrossRef](#)] [[PubMed](#)]
27. Zhao, Y.; Abdullayev, E.; Vasiliev, A.; Lvov, Y. Halloysite nanotubule clay for efficient water purification. *J. Colloid Interface Sci.* **2013**, *406*, 121–129. [[CrossRef](#)] [[PubMed](#)]
28. Cavallaro, G.; Danilushkina, A.A.; Evtugyn, V.G.; Lazzara, G.; Milioto, S.; Parisi, F.; Rozhina, E.V.; Fakhrullin, R.F. Halloysite Nanotubes: Controlled Access and Release by Smart Gates. *Nanomaterials* **2017**, *7*, 199. [[CrossRef](#)] [[PubMed](#)]
29. Cavallaro, G.; Lazzara, G.; Milioto, S.; Parisi, F.; Ruisi, F. Nanocomposites based on esterified colophony and halloysite clay nanotubes as consolidants for waterlogged archaeological woods. *Cellulose* **2017**, *24*, 3367–3376. [[CrossRef](#)]
30. Cavallaro, G.; Lazzara, G.; Milioto, S.; Parisi, F.; Sparacino, V. Thermal and dynamic mechanical properties of beeswax-halloysite nanocomposites for consolidating waterlogged archaeological woods. *Polym. Degrad. Stab.* **2015**, *120*, 220–225. [[CrossRef](#)]
31. Cavallaro, G.; Lazzara, G.; Milioto, S.; Parisi, F. Halloysite nanotubes as sustainable nanofiller for paper consolidation and protection. *J. Therm. Anal. Calorim.* **2014**, *117*, 1293–1298. [[CrossRef](#)]
32. Cavallaro, G.; Lazzara, G.; Milioto, S.; Parisi, F. Halloysite Nanotubes for Cleaning, Consolidation and Protection. *Chem. Rec.* **2018**. [[CrossRef](#)] [[PubMed](#)]
33. Gorrasi, G. Dispersion of halloysite loaded with natural antimicrobials into pectins: Characterization and controlled release analysis. *Carbohydr. Polym.* **2015**, *127*, 47–53. [[CrossRef](#)] [[PubMed](#)]
34. Thill, A.; Maillet, P.; Guiose, B.; Spalla, O.; Belloni, L.; Chaurand, P.; Auffan, M.; Olivi, L.; Rose, J. Physico-chemical Control over the Single- or Double-Wall Structure of Aluminogermanate Imogolite-like Nanotubes. *J. Am. Chem. Soc.* **2012**, *134*, 3780–3786. [[CrossRef](#)] [[PubMed](#)]
35. Rotoli, B.M.; Guidi, P.; Bonelli, B.; Bernardeschi, M.; Bianchi, M.G.; Esposito, S.; Frenzilli, G.; Lucchesi, P.; Nigro, M.; Scarcelli, V.; et al. Imogolite: An Aluminosilicate Nanotube Endowed with Low Cytotoxicity and Genotoxicity. *Chem. Res. Toxicol.* **2014**, *27*, 1142–1154. [[CrossRef](#)] [[PubMed](#)]
36. Cradwick, P.D.G.; Farmer, V.C.; Russell, J.D.; Masson, C.R.; Wada, K.; Yoshinaga, N. Imogolite, a Hydrated Aluminium Silicate of Tubular Structure. *Nat. Phys. Sci.* **1972**, *240*, 187–189. [[CrossRef](#)]
37. Amara, M.-S.; Paineau, E.; Bacia-Verloop, M.; Krapf, M.-E.M.; Davidson, P.; Belloni, L.; Levard, C.; Rose, J.; Launois, P.; Thill, A. Single-step formation of micron long (OH)₃Al₂O₃Ge(OH) imogolite-like nanotubes. *Chem. Commun.* **2013**, *49*, 11284–11286. [[CrossRef](#)] [[PubMed](#)]
38. Rubio, A.; Corkill, J.L.; Cohen, M.L. Theory of graphitic boron nitride nanotubes. *Phys. Rev. B* **1994**, *49*, 5081–5084. [[CrossRef](#)]
39. Chopra, N.G.; Luyken, R.J.; Cherrey, K.; Crespi, V.H.; Cohen, M.L.; Louie, S.G.; Zettl, A. Boron Nitride Nanotubes. *Science* **1995**, *269*, 966–967. [[CrossRef](#)] [[PubMed](#)]
40. Madani, M.S.; Monajjemi, M.; Aghaei, H. The Double Wall Boron Nitride Nanotube: Nano-Cylindrical Capacitor. *Orient. J. Chem.* **2017**, *33*, 1213–1222. [[CrossRef](#)]

41. Chopra, N.G.; Zettl, A. Measurement of the elastic modulus of a multi-wall boron nitride nanotube. *Solid State Commun.* **1998**, *105*, 297–300. [[CrossRef](#)]
42. Zhi, C.; Bando, Y.; Tang, C.; Xie, R.; Sekiguchi, T.; Golberg, D. Perfectly dissolved boron nitride nanotubes due to polymer wrapping. *J. Am. Chem. Soc.* **2005**, *127*, 15996–15997. [[CrossRef](#)] [[PubMed](#)]
43. Terao, T.; Zhi, C.; Bando, Y.; Mitome, M.; Tang, C.; Golberg, D. Alignment of Boron Nitride Nanotubes in Polymeric Composite Films for Thermal Conductivity Improvement. *J. Phys. Chem. C* **2010**, *114*, 4340–4344. [[CrossRef](#)]
44. Ciofani, G.; Danti, S.; Ricotti, L.; D'Alessandro, D.; Moscato, S.; Berrettini, S.; Mattoli, V.; Menciasci, A. Boron nitride nanotubes: Production, properties, biological interactions and potential applications as therapeutic agents in brain diseases. *Curr. Nanosci.* **2011**, *7*. [[CrossRef](#)]
45. Gao, Z.; Zhi, C.; Bando, Y.; Golberg, D.; Serizawa, T. Chapter 2—Functionalization of boron nitride nanotubes for applications in nanobiomedicine. In *Boron Nitride Nanotubes in Nanomedicine*; Elsevier Inc.: New York, NY, USA, 2016; pp. 17–40.
46. Ciofani, G.; Genchi, G.G.; Liakos, I.; Athanassiou, A.; Dinucci, D.; Chiellini, F.; Mattoli, V. A simple approach to covalent functionalization of boron nitride nanotubes. *J. Colloid Interface Sci.* **2012**, *374*. [[CrossRef](#)] [[PubMed](#)]
47. Li, X.; Hanagata, N.; Wang, X.; Yamaguchi, M.; Yi, W.; Bando, Y.; Golberg, D. Multimodal luminescent-magnetic boron nitride nanotubes@NaGdF(4):Eu structures for cancer therapy. *Chem. Commun.* **2014**, *50*, 4371–4374. [[CrossRef](#)] [[PubMed](#)]
48. Ferreira, T.H.; Hollanda, L.M.; Lancellotti, M.; de Sousa, E.M.B. Boron nitride nanotubes chemically functionalized with glycol chitosan for gene transfection in eukaryotic cell lines. *J. Biomed. Mater. Res. Part A* **2015**, *103*, 2176–2185. [[CrossRef](#)] [[PubMed](#)]
49. Şen, Ö.; Çulha, M. Boron nitride nanotubes included thermally cross-linked gelatin-glucose scaffolds show improved properties. *Colloids Surf. B* **2016**, *138*, 41–49. [[CrossRef](#)] [[PubMed](#)]
50. Yu, Y.; Chen, H.; Liu, Y.; Li, L.H.; Chen, Y. Humidity sensing properties of single Au-decorated boron nitride nanotubes. *Electrochem. Commun.* **2013**, *30*, 29–33. [[CrossRef](#)]
51. Leela, A.; Reddy, M.; Tanur, A.E.; Walker, G.C. Synthesis and hydrogen storage properties of different types of boron nitride nanostructures. *Int. J. Hydrogen Energy* **2010**, *35*, 4138–4143. [[CrossRef](#)]
52. Cavallaro, G.; Grillo, I.; Gradzielski, M.; Lazzara, G. Structure of Hybrid Materials Based on Halloysite Nanotubes Filled with Anionic Surfactants. *J. Phys. Chem. C* **2016**, *120*, 13492–13502. [[CrossRef](#)]
53. Luo, Z.; Song, H.; Feng, X.; Run, M.; Cui, H.; Wu, L.; Gao, J.; Wang, Z. Liquid Crystalline Phase Behavior and Sol-Gel Transition in Aqueous Halloysite Nanotube Dispersions. *Langmuir* **2013**, *29*, 12358–12366. [[CrossRef](#)] [[PubMed](#)]
54. Bertolino, V.; Cavallaro, G.; Lazzara, G.; Milioto, S.; Parisi, F. Biopolymer-Targeted Adsorption onto Halloysite Nanotubes in Aqueous Media. *Langmuir* **2017**, *33*, 3317–3323. [[CrossRef](#)] [[PubMed](#)]
55. Lee, Y.; Jung, G.-E.; Cho, S.J.; Geckeler, K.E.; Fuchs, H. Cellular interactions of doxorubicin-loaded DNA-modified halloysite nanotubes. *Nanoscale* **2013**. [[CrossRef](#)] [[PubMed](#)]
56. Cavallaro, G.; Lazzara, G.; Milioto, S. Exploiting the Colloidal Stability and Solubilization Ability of Clay Nanotubes/Ionic Surfactant Hybrid Nanomaterials. *J. Phys. Chem. C* **2012**, *116*, 21932–21938. [[CrossRef](#)]
57. Cavallaro, G.; Lazzara, G.; Milioto, S.; Parisi, F. Steric stabilization of modified nanoclays triggered by temperature. *J. Colloid Interface Sci.* **2016**, *461*, 346–351. [[CrossRef](#)] [[PubMed](#)]
58. Cavallaro, G.; Lazzara, G.; Massaro, M.; Milioto, S.; Noto, R.; Parisi, F.; Riela, S. Biocompatible Poly(*N*-isopropylacrylamide)-halloysite Nanotubes for Thermoresponsive Curcumin Release. *J. Phys. Chem. C* **2015**, *119*, 8944–8951. [[CrossRef](#)]
59. Cavallaro, G.; Lazzara, G.; Milioto, S.; Parisi, F.; Sanzillo, V. Modified Halloysite Nanotubes: Nanoarchitectures for Enhancing the Capture of Oils from Vapor and Liquid Phases. *ACS Appl. Mater. Interfaces* **2014**, *6*, 606–612. [[CrossRef](#)] [[PubMed](#)]
60. Derjaguin, B.V.; Landau, L.D. Theory of the Stability of Strongly Charged Lyophobic Sols and of the Adhesion of Strongly Charged Particles in Solutions of Electrolytes. *Acta Physicochim.* **1941**, *14*, 733–762. [[CrossRef](#)]
61. Cavallaro, G.; Lazzara, G.; Milioto, S.; Palmisano, G.; Parisi, F. Halloysite nanotube with fluorinated lumen: Non-foaming nanocontainer for storage and controlled release of oxygen in aqueous media. *J. Colloid Interface Sci.* **2014**, *417*, 66–71. [[CrossRef](#)] [[PubMed](#)]

62. Lun, H.; Ouyang, J.; Yang, H. Enhancing dispersion of halloysite nanotubes via chemical modification. *Phys. Chem. Miner.* **2014**, *41*, 281–288. [[CrossRef](#)]
63. Chang, P.R.; Xie, Y.; Wu, D.; Ma, X. Amylose wrapped halloysite nanotubes. *Carbohydr. Polym.* **2011**, *84*, 1426–1429. [[CrossRef](#)]
64. Shamsi, M.H.; Geckeler, D.V. The first biopolymer-wrapped non-carbon nanotubes. *Nanotechnology* **2008**, *19*, 075604. [[CrossRef](#)] [[PubMed](#)]
65. Cavallaro, G.; Lazzara, G.; Milioto, S.; Parisi, F. Hydrophobically Modified Halloysite Nanotubes as Reverse Micelles for Water-in-Oil Emulsion. *Langmuir* **2015**, *31*, 7472–7478. [[CrossRef](#)] [[PubMed](#)]
66. Du, P.; Yuan, P.; Thill, A.; Annabi-Bergaya, F.; Liu, D.; Wang, S. Insights into the formation mechanism of imogolite from a full-range observation of its sol-gel growth. *Appl. Clay Sci.* **2017**, *150*, 115–124. [[CrossRef](#)]
67. Kanji, K.; Nobuo, D.; Yuzuru, H.; Hiroshi, I. Lyotropic mesophase of imogolite, 1. Effect of polydispersity on phase diagram. *Makromol. Chem.* **1986**, *187*, 2883–2893. [[CrossRef](#)]
68. Livolant, F.; Leforestier, A. Condensed phases of DNA: Structures and phase transitions. *Prog. Polym. Sci.* **1996**, *21*, 1115–1164. [[CrossRef](#)]
69. Vroege, G.J.; Thies-Weesie, D.M.E.; Petukhov, A.V.; Lemaire, B.J.; Davidson, P. Smectic Liquid-Crystalline Order in Suspensions of Highly Polydisperse Goethite Nanorods. *Adv. Mater.* **2006**, *18*, 2565–2568. [[CrossRef](#)]
70. Ramos, L.; Fabre, P. Swelling of a lyotropic hexagonal phase by monitoring the radius of the cylinders. *Langmuir* **1997**, *13*, 682–685. [[CrossRef](#)]
71. Karube, J. Hysteresis of the Colloidal Stability of Imogolite. *Clays Clay Miner.* **1998**, *46*, 583–585. [[CrossRef](#)]
72. Ma, Y.L.; Karube, J. Imogolite flocculation under alkaline conditions. *Soil Sci. Plant Nutr.* **2013**, *59*, 125–129. [[CrossRef](#)]
73. Gao, Z.; Zhi, C.; Bando, Y.; Golberg, D.; Serizawa, T. Noncovalent Functionalization of Boron Nitride Nanotubes in Aqueous Media Opens Application Roads in Nanobiomedicine. *Nanobiomedicine* **2014**, *1*, 7. [[CrossRef](#)]
74. Kim, D.; Sawada, T.; Zhi, C.Y.; Bando, Y.; Golberg, D.; Serizawa, T. Dispersion of Boron Nitride Nanotubes in Aqueous Solution by Simple Aromatic Molecules. *J. Nanosci. Nanotechnol.* **2014**, *14*, 3028–3033. [[CrossRef](#)] [[PubMed](#)]
75. Gao, Z.; Fujioka, K.; Sawada, T.; Zhi, C.; Bando, Y.; Golberg, D.; Aizawa, M.; Serizawa, T. Noncovalent functionalization of boron nitride nanotubes using water-soluble synthetic polymers and the subsequent preparation of superhydrophobic surfaces. *Polym. J.* **2013**, *45*, 567–570. [[CrossRef](#)]
76. Wu, X.; An, W.; Zeng, X.C. Chemical functionalization of boron-nitride nanotubes with NH₃ and amino functional groups. *J. Am. Chem. Soc.* **2006**, *128*, 12001–12006. [[CrossRef](#)] [[PubMed](#)]
77. Lau, Y.T.R.; Yamaguchi, M.; Li, X.; Bando, Y.; Golberg, D.; Winnik, F.M. Facile and mild strategy toward biopolymer-coated boron nitride nanotubes via a glycine-assisted interfacial process. *J. Phys. Chem. C* **2013**, *117*, 19568–19576. [[CrossRef](#)]
78. Gao, Z.; Zhi, C.; Bando, Y.; Golberg, D.; Komiyama, M.; Serizawa, T. Efficient disentanglement of boron nitride nanotubes using water-soluble polysaccharides for protein immobilization. *RSC Adv.* **2012**, *2*, 6200–6208. [[CrossRef](#)]
79. Gao, Z.; Zhi, C.; Bando, Y.; Golberg, D.; Serizawa, T. Isolation of individual boron nitride nanotubes via peptide wrapping. *J. Am. Chem. Soc.* **2010**, *132*, 4976–4977. [[CrossRef](#)] [[PubMed](#)]
80. Gao, Z.; Zhi, C.; Bando, Y.; Golberg, D.; Serizawa, T. Noncovalent functionalization of disentangled boron nitride nanotubes with flavin mononucleotides for strong and stable visible-light emission in aqueous solution. *ACS Appl. Mater. Interfaces* **2011**, *3*, 627–632. [[CrossRef](#)] [[PubMed](#)]
81. Zhi, C.; Bando, Y.; Wang, W.; Tang, C.; Kuwahara, H.; Golberg, D. DNA-mediated assembly of boron nitride nanotubes. *Chem. Asian J.* **2007**, *2*, 1581–1585. [[CrossRef](#)] [[PubMed](#)]
82. Emanet, M.; Şen, Ö.; Çulha, M. Evaluation of boron nitride nanotubes and hexagonal boron nitrides as nanocarriers for cancer drugs. *Nanomedicine* **2017**, *12*, 797–810. [[CrossRef](#)] [[PubMed](#)]
83. Lee, C.; Zhang, D.; Yap, Y. Functionalization, Dispersion, and Cutting of Boron Nitride Nanotubes in Water. *J. Phys. Chem. C* **2012**, *116*, 1798–1804. [[CrossRef](#)]
84. Ikuno, T.; Sainsbury, T.; Okawa, D.; Frechet, J.M.J.; Zettl, A. Amine-functionalized boron nitride nanotubes. *Solid State Commun.* **2007**, *142*, 643–646. [[CrossRef](#)]

85. Zhi, C.; Bando, Y.; Tang, C.; Honda, S.; Sato, K.; Kuwahara, H.; Golberg, D. Covalent functionalization: Towards soluble multiwalled boron nitride nanotubes. *Angew. Chem. Int. Ed.* **2005**, *44*, 7932–7935. [[CrossRef](#)] [[PubMed](#)]
86. Emanet, M.; Şen, Ö.; Çobandede, Z.; Çulha, M. Interaction of carbohydrate modified boron nitride nanotubes with living cells. *Colloids Surf. B* **2015**, *134*, 440–446. [[CrossRef](#)] [[PubMed](#)]
87. Şen, Ö.; Çobandede, Z.; Emanet, M.; Bayrak, Ö.F.; Çulha, M. Boron nitride nanotubes for gene silencing. *Biochim. Biophys. Acta Gen. Subj.* **2017**, *1861*, 2391–2397. [[CrossRef](#)] [[PubMed](#)]
88. Zhi, C.Y.; Bando, Y.; Terao, T.; Tang, C.C.; Kuwahara, H.; Golberg, D. Chemically activated boron nitride nanotubes. *Chem. Asian J.* **2009**, *4*, 1536–1540. [[CrossRef](#)] [[PubMed](#)]
89. Lin, S.; Ashrafi, B.; Laqua, K.; Kim, S. Nanotubes with peroxides and their application in polycarbonate composites. *New J. Chem.* **2017**, *41*, 7571–7577. [[CrossRef](#)]
90. Ejaz, M.; Rai, S.C.; Wang, K.; Zhang, K.; Zhou, W.; Grayson, S.M. Surface-initiated atom transfer radical polymerization of glycidyl methacrylate and styrene from boron nitride nanotubes. *J. Mater. Chem. C* **2014**, *2*, 4073–4079. [[CrossRef](#)]
91. Stetsyshyn, Y.; Raczowska, J.; Lishchynskiy, O.; Bernasik, A.; Kostruba, A.; Harhay, K.; Ohar, H.; Marzec, M.M.; Budkowski, A. Temperature-Controlled Three-Stage Switching of Wetting, Morphology, and Protein Adsorption. *ACS Appl. Mater. Interfaces* **2017**, *9*, 12035–12045. [[CrossRef](#)] [[PubMed](#)]
92. Raczowska, J.; Stetsyshyn, Y.; Awsiuk, K.; Zemła, J.; Kostruba, A.; Harhay, K.; Marzec, M.; Bernasik, A.; Lishchynskiy, O.; Ohar, H.; Budkowski, A. Temperature-responsive properties of poly(4-vinylpyridine) coatings: Influence of temperature on the wettability, morphology, and protein adsorption. *RSC Adv.* **2016**, *6*, 87469–87477. [[CrossRef](#)]
93. Lin, Y.; Williams, T.V.; Cao, W.; Elsayed-Ali, H.E.; Connell, J.W. Defect functionalization of hexagonal boron nitride nanosheets. *J. Phys. Chem. C* **2010**, *114*, 17434–17439. [[CrossRef](#)]
94. Sundaram, R.; Scheiner, S.; Roy, A.K.; Kar, T. B=N bond cleavage and BN ring expansion at the surface of boron nitride nanotubes by iminoborane. *J. Phys. Chem. C* **2015**, *119*, 3253–3259. [[CrossRef](#)]



© 2018 by the authors. Licensee MDPI, Basel, Switzerland. This article is an open access article distributed under the terms and conditions of the Creative Commons Attribution (CC BY) license (<http://creativecommons.org/licenses/by/4.0/>).